Characterisation of black skin stratum corneum by digital macroscopic images analysis

Géraud M. Azehoun-Pazou[1,2] ✉, *Kokou M. Assogba*[2], *Hugues Adegbidi*[3], *Antoine C. Vianou*[2,4]

[1]*National University of Sciences, Technologies, Engineering and Mathematics (UNSTIM), BP 2282 Abomey, Benin*
[2]*Laboratory of Electrical Engineering, Telecommunications and Applied Informatics (LETIA), University of Abomey-Calavi, 01 BP 2009, Abomey-Calavi, Benin*
[3]*Department of Dermatology and Venerology, Faculty of Health Sciences, University of Abomey-Calavi, 01 BP 188, Abomey-Calavi, Benin*
[4]*Laboratory of Thermophysical Characterization and Energetic Appropriation (Lab-CTMAE), Polytechnic School of Abomey-Calavi, 01 BP 2009, Abomey-Calavi, Benin*
✉ *E-mail: geraud.pazou@unstim.bj*

Published in Healthcare Technology Letters; Received on 29th June 2020; Revised on 2nd November 2020; Accepted on 10th November 2020

Black skin medical images generally show very low contrast. Being in a global initiative of characterisation of black skin horny layer (stratum corneum) by digital images analysis, the authors in this study proposed a four-step approach. The first step consists of differentiation between probable healthy skin regions and those affected. For that, they used an automatic classification system based on multilayer perceptron artificial neural networks. The network has been trained with texture and colour features. Best features selection and network architecture definition were done using sequential network construction algorithm-based method. After classification, selected regions undergo a colour transformation, in order to increase the contrast with the lesion region. Thirdly, created colour information serves as the basis for a modified fuzzy c-mean clustering algorithm to perform segmentation. The proposed method, named neural network-based fuzzy clustering, was applied to many black skin lesion images and they obtained segmentation rates up to 94.67%. The last stage consists in calculating characteristics. Eight parameters are concerned: uniformity, standard deviation, skewness, kurtosis, smoothness, entropy, and average pixel values calculated for red and blue colour channels. All developed methods were tested with a database of 600 images and obtained results were discussed and compared with similar works.

1. Introduction: This paper is an extension of a work originally presented in [1]. Whereas previously, we proposed a new approach of segmentation for black skin digital macroscopic images, here we propose a complete analysis process that leads to the characterisation of lesions and pigmented disorders. Dermatology is one of the fields where medical images have been used for years since their potential benefits had been revealed. Different methods, techniques, approaches and theories have been developed over the years and were applied to different types of images and lesions (or dermatosis) for which they provided good tools for self-detection, analysis and characterisation [2–6]. As an illustration, characteristics (features calculated from images) have been identified and used as part of the skin lesion discrimination pipeline for early melanoma cancer diagnosis by [7]. Moreover, recent advances in deep learning show very promising results as it is able to improve existing pipeline performance [6]. Despite these remarkable advances, there is very few information about black skin description with some specific characteristics. Actually, very few works were done specifically on black skin, in terms of digital image analysis. However, characterisation can help in early identification of skin changes as well as particular structures which may be specific to types of lesion. Therefore, there is a need to provide tools and methods that can serve as support for computer-assisted decision-making.

Image analysis regroups all operations that aim to describe images with some characteristics. It generally goes through the following steps: identification of the region of interest (ROI), extraction of features and selection of features (characteristics). ROI identification often starts with preprocessing followed by segmentation. So, the generally adopted image analysis process includes the following steps: pre-processing, segmentation, extraction and selection of features [8]. Generally, in skin images, there are many parameters such as type and quality of images, noise, acquisition techniques, which influence image analysis. As an illustration, black skin images are certainly the one for which segmentation is the most difficult because of the low contrast between safe and abnormal skin regions (cf. Fig. 1). Skin colour is black when there is a high concentration of melanocyte cells in its basal layer. Such a fact makes image acquisition techniques like dermoscopy and other equipment inefficient in black skin, and then unusable by specialists. Black skin specialists are therefore limited to macroscopic images.

Analysing black skin macroscopic images is a challenging task. Even though there is no specific work on black skin, there exist many performant methods and approaches for each step. As far as pre-processing is concerned, several approaches exist to eliminate noise and hairs as such as peer group filter [9, 10], the mean filters and the median filter [8, 11–14], Gaussian filters [15]. However, most of these techniques often result either in an unwanted blur, or disturbances of texture in images or colour changes. As solutions to these problems, methods that can automatically detect artefacts and remove them have been exposed in [1, 16, 17] and they showed their effectiveness. Concerning segmentation, which is a very important step, there is no universal method. Generally, the choice of one approach over another usually depends on intended applications. However, we noticed that model-based approaches used in and those based on artificial intelligence algorithms are among the most used nowadays. About feature extraction and selection methods, artificial neural networks (ANN), decision trees and SVM (support vector machine) are among the most appreciated.

Our goals in this work is to propose mathematical and algorithmic methods suitable for black skin macroscopic images processing, in order to characterise the surface of the stratum corneum. Achievement of this goal includes:

- selection of features from images;
- development of image processing algorithms aiming on the one hand to automatically identify ROIs in images and

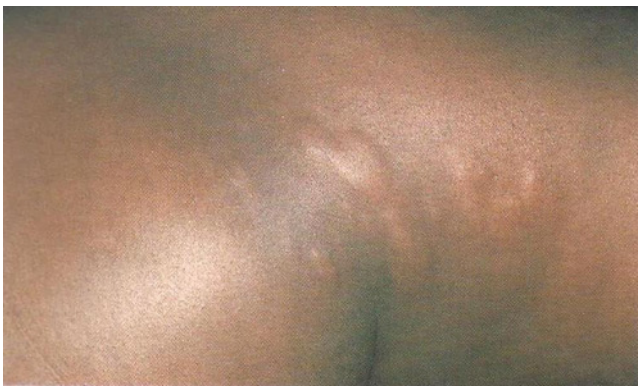

Fig. 1 *Macroscopic image of black skin showing lesion (source: [10])*

Table 1 Images database composition

Categories or types	Number of images
Erythema	24
Recklinghausen neurofibromatosis	20
Purpura lesion	21
Seborrheic keratosis	23
Eczema	22
healthy skin parts of body	60
scanned lesionor p.d. images	50

on the other hand to calculate on these regions selected characteristics;
- evaluate the proposed methods and compare them to the existing.

The rest of the paper is organised as follows: Section 2 presents the materials used in this work; Section 3 presents the methods used in this work; Section 4 presents our results; in Section 5 we present a discussion and finally we conclude in Section 6.

2. Material: All macroscopic images of the surface of the horny layer of the skin (stratum corneum) were used in our work. We have a database of 300 images. In Table 1, details about database composition are presented and Fig. 2 shows some of the images. Images in the database are of size 2048×1536 (definition is then 3 megapixels).

The database is composed as follows:

- images of lesions and pigmented disorders captured with a digital camera, in the Dermatology service of the Hubert Maga University Hospital (CNHU-HKM) of Cotonou;
- scanned images of lesions and pigmented disorders;
- images of different healthy skin parts of the body;
- images downloaded from online databases.

Images downloaded from online databases include some white skin types. Indeed, we browsed many online image databases such as dermnet.com, dermatologie.free.fr, vulgaris-medical.com. Even though they rarely contain images showing skin colours ranging from matte to black, we were able to extract some, in order to test algorithms. Our algorithms were implemented in MATLAB, version 9.0 (R2016a). We mainly use 'Image Processing' and 'Neural Network Toolbox' libraries.

3. Method: In this section, we present methods we used and the ones we developed as part of the proposed image analysis process. Section 3.1 presents features' selection. In Section 3.2,

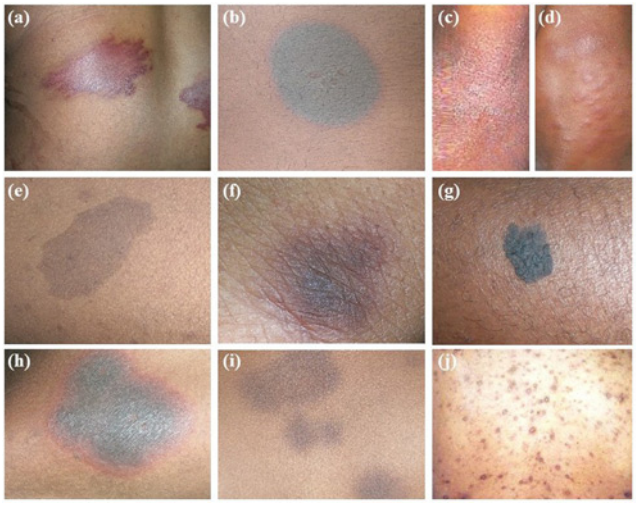

Fig. 2 *Sample of some images of our database*
a Purpura lesion
b, d, f, h, i Different types of erythema
c, j Eczema
e Recklinghausen neurofibromatosis
g Seborrheic keratosis

we explain the proposed segmentation method which is named NNFC (neural network-based fuzzy clustering). It is a combination of classification and fuzzy clustering.

3.1. Selection of black skin characteristics: The purpose of feature selection is to identify features that could be calculated to describe the texture and the colour of the skin and thus being able to identify early changes. This is a problem of 'differentiation between lesion areas and healthy skin areas'. An 'area' corresponds here to a block of pixels that belong to any region of the image. It is, therefore, a problem of classification of a given area of the image, as belonging to lesion region or healthy ones. Classification makes it possible to identify a pattern from raw data in order to make a decision depending on the category assigned to that pattern [13]. Here, we try to recognise not only geometric patterns but more generally any pattern contained in images. Various machine learning algorithms can be used, such as neural networks, statistical analysis, hidden Markov models, isomorphism search of graphs or sub-graphs. Among these methods, we opted for neural networks.

The best neural network architecture selection was done by searching the space of possible architectures. We retain two layers' perceptron's architecture characterised by the number of hidden units and the number of input variables. Input variables are texture and colour parameters extracted from blocks in segmented images. Therefore, there are up to ten input variables (uniformity, asymmetry, entropy, contrast or standard deviation, skewness, kurtosis, mean pixel values in R, G, B colour channels and also greyscale).

To construct all these possible networks, we use SNC (sequential network construction) algorithm. However, since at the output layer we have two neurons, we chose to have at least two more neurons going up to the input layer. Thus, we started with a network of six input neurons and four neurons in the hidden layer, to successively evolve up to ten neurons in input and ten in the hidden layer. This choice is driven by the desire to have at each combination, both colour and texture information present in the network architecture. In absence of any a priori rule that says how to choose the number of neurons in the hidden layer and the input layer, depending on the two neurons in the output layer, we should search over all possibilities. To avoid that, we used a search strategy inspired by

the one proposed in [14]. It is a pruning method for input methods like SBP (sensitivity-base pruning). However, here the decision criterion is FMR (false match rate) associated with a possible network after learning. The choice of FMR is driven by the desire to consider both types of misclassification as a decision criterion.

3.1.1 Colour features: We calculate the mean intensity value for each of the R, G and B channels ($M_{R,}$ $M_{G,}$ M_B) and also grey level 'M_{Gr}' with formula (1). For each block of pixels X (3,3) and '$z(i)$' any value of pixel intensity in X, we have:

$$M_k = \frac{1}{9}\sum_{i=1}^{3}\sum_{j=1}^{3} X(i,j),\ \ k = \{\mathrm{R, G, B, G}_r\}. \tag{1}$$

3.1.2 Texture features: They were chosen for their pertinence and efficiency regarding classification performance achieved with them. They are uniformity, entropy, kurtosis, regularity, asymmetry and standard deviation.

- *Uniformity U:* This is the expression of a certain harmony, in the pixel block, in terms of the pixel intensity distribution. It is maximum when all grey levels are equal (maximum uniformly). Also known as energy or angular second moment, it is calculated using formula (2).
- *Entropy e:* A measure of the randomness of the intensity distribution. It is calculated using formula (3).
- *Kurtosis K:* This is the measure of the distribution of the distribution of pixel intensities. It is calculated using formula (4).
- *The regularity r:* Its value is 0 for regions of constant intensity and approaches 1 for regions with large variations in intensity level values. It is calculated using formula (5).
- *Asymmetry:* This is the measure of the variation of the intensity values around the average intensity. It is calculated using formula (6).
- *Standard deviation or contrast σ:* It measures here the average contrast of the zone. It is calculated using formula (7).

$$U = \sum_{i=1}^{l} p^2(z_{i0}) \tag{2}$$

$$\sigma = \sum_{i=1}^{l} (z_i - m)^2 p(z_i) \tag{3}$$

$$s = \sum_{i=1}^{l} (z_i - m)^3 p(z_i) \tag{4}$$

$$r = 1 - \frac{1}{1+\sigma^2} \tag{5}$$

$$K = \sum_{i=1}^{l} (z_i - m)^4 p(z_i) \tag{6}$$

$$e = -\sum_{i=1}^{l} p(z_i)\log_2 p(z_i) \tag{7}$$

where l is the number of possible intensity levels, z_i is a random value of pixel intensity, $p(z)$ is the histogram of intensity levels in a region, and m the average intensity defined by formula (8):

$$m = \sum_{i=1}^{l} z_i p(z_i). \tag{8}$$

3.2. Segmentation by NNFC method: We propose as segmentation method, a fuzzy clustering based on a neural network classifier. This method, named neural network-based fuzzy clustering (NNFC) helps to automatically circumcise the ROI. It proceeds in three steps, such as:

- classification by a system based on neural networks multilayer perceptron (MLP), developed for this purpose;
- colour transformation followed by a smoothing;
- finally, segmentation by clustering.

3.2.1 Colour transform: The aim of colour transformation is to increase the contrast between healthy skin regions and lesion regions. To do this, we thought that it could function as a translation from a departure pixel intensity interval '***Dp***' to an arrival intensity interval '***Ar***'. '***Dp***' is a vector obtained by extracting the histogram of the concerned image, focusing only on pixels classified as belonging to healthy skin; '***Ar***' is a histogram obtained from reference white skin images. To transform image, we seek to determine the transformation coefficients (α, β, γ) of linear equations (9) (10) and (12), respectively, where 'Pixel value' is the pixel value representative of ***Dp*** and 'Value of ref' is the pixel value representative of ***Ar***.

$$\begin{cases} \text{Pixel value}_R = \text{Value of ref} + \alpha \\ \text{Pixel value}_G = \text{Value of ref} + \gamma \\ \text{Pixel value}_B = \text{Value of ref} + \beta \end{cases} \tag{9-11}$$

$$\frac{1}{n}\sum_{i,j}\frac{1}{\delta_{Ar}\delta_{Dp}}\left(Ar(i,j) - \overline{Dp}\right)\left(Dp(i,j) - \overline{Ar}\right). \tag{12}$$

To obtain, α, β and γ we compute the inter-correlation (or cross-correlation) of the two vectors ***Ar*** and ***Dp***, given by formula (12). Thus, each pixel *P(i,j)* with colour channel values *R(i,j) G(i,j)* and *B(i,j)* is replaced by a value *P′(i,j)* with corresponding colour channel values *R′(i,j) G′(i,j)* and *B′(i,j)* such as:

$$\begin{cases} R'_{i,j} = R_{i,j} + \alpha \\ G'_{i,j} = G_{i,j} + \gamma \\ B'_{i,j} = B_{i,j} + \beta \end{cases} \tag{13-15}$$

The colour transformation uses non-linear interpolation functions that associate with each initial value of intensity a final value. As a result, inter-block discontinuities may appear at the transformed image. To correct them, we make a morphological opening followed by a medium filtering. The opening makes it possible to soften the contours, cut the narrow isthmus, remove small islands and narrow headlands. Isthmus, islands and capes are discontinuities observable within images. The opening of an image X by a structuring element B is carried out by performing an erosion by B followed by a dilation by the transpose B' of B (that is to say the symmetry of B with respect to its centre), which is:

$$O^B(X) = D^{B'}\left(E^B(X)\right). \tag{16}$$

3.2.2 Creating cluster by modified fuzzy c-mean (FCM) algorithm: Clustering consists of automatically grouping the pixels of the image into natural clusters, without any prior knowledge of the probable classes (or clusters) to which they could belong [18]. These clusters are characterised by a strong similarity within and a strong dissimilarity between members of different groups. For this purpose, clustering methods are based on the notion of distance between the objects of the image, assuming that if two objects are close according to this distance, they must be grouped together in the same cluster. Among the clustering methods most used in segmentation, we find the *k*-means and the FCM. The FCM in particular had the best performance in view of the experimental

results obtained. Our choice was therefore focused on this algorithm, which we modified to make it faster and more appropriate in our context. The algorithm uses a vector, which contains pixel values of the image to be segmented. The algorithm proceeds by partitioning into c clusters, data provided to it, minimising an 'objective function' of quadratic error. Let J_{FC} be this function; J_{FC} is defined by formula (17). In this formula, $X = \{x_1, x_2, \ldots, x_n\} \subseteq R^n$ is the set of input data to group, n is the number of elements of X. In addition, c is the number of clusters, 'u_{ik}' represents the degree of membership of 'x_k' to the ith cluster, 'q' is a weighting exponent of the degree of membership of x_k to ith cluster, v_i is the centre of cluster 'i', $d(x_k, v_i)$ is a measure of distance between object 'x_k' and the centre 'v_i' of ith cluster

$$J_{FC} = \sum_{k=1}^{n} \sum_{i=1}^{c} (u_{ik})^q d^2(x_k, v_i). \tag{17}$$

The formulation of 'objective function J_{FC}' that we present in formula (17) differs from that of the original formulation. Indeed, the Euclidean distance is used in the classical FCM algorithm whereas here, we use instead the Chebyshev distance (also called 'Queen-wise' distance) defined by formula (18) where A and B are two points respective coordinates (A_0, …, A_N) and (B_0, …, B_N). The choice of this method is justified by the fact that one seeks, through the calculation of a distance metric, to determine the position of a pixel of the image with respect to the centre of a cluster, which is also a pixel. Therefore, it is better to consider the greater distance between those obtained by following the vertical axis and the horizontal axis, because we are on a 2D plane (so $N = 2$). Moreover, this choice would make the algorithm go faster in making decisions about membership of a cluster or another. All these considerations made, the solution of objective function JFC is obtained by an iterative process detailed in [15]

$$dT(A, B) = \max_{i \in [0,N]} \|A_i - B_i\|. \tag{18}$$

Once images are segmented, each lesion is characterised by selected features.

4. Results: At the end of the features selection process, the best learning performance was obtained with eight input layer variables out of the ten initially extracted. Following eight characteristics were selected: uniformity, skewness, kurtosis, smoothness, entropy, contrast, and mean pixel values calculated for red and blue colour channels. Note that the number of hidden layer neurons associated with this input is nine. With such configuration, the network reached its best validation performance from 457th iteration where objective function's entropy value was about 0.083 but the algorithm stopped at iteration 463. The FMR associated with this configuration is 2.7% in both learning, validation and testing phases. This result corresponds to 2.9% of misclassified normal skin regions, while only 2.4% of lesion areas were misclassified.

Fig. 3 shows segmented images of some lesions. Table 2 presents the ranges of texture parameters values calculated for randomly selected 150 lesion images of our database. When we consider texture characteristics values of all lesion images in our database and compare them to those obtained with healthy skin images, we obtain the graphics of Figs. 4–9.

A study of Figs. 4–7 reveals that values obtained for contrast (or standard deviation), smoothness, kurtosis and uniformity, respectively on lesion images and healthy skin, vary in distinct ranges. From this observation, we can say that the calculated characteristics can help in differentiating lesion areas from healthy skin. From Figs. 8 and 9, we can say that value ranges of skewness and entropy are also distant, though they are close for some lesions images. As a general conclusion, we can say that if all selected characteristics are combined, they can be good indicators of the existence or not of lesions in a stratum corneum image.

5. Discussion: The aim of characterisation is to determine features which can help to identify a particular type of lesion or to differentiate lesions between themselves. Research in this domain is very active, especially for early detection of skin cancers like melanoma. Works done in [7, 16] are of particular interest in this context. While in [16], wavelet transform is used to model lesions boundary irregularity, in [7] innovative pixels' values-based features were extracted from the ROI. Features used by authors in [7] are of the same type than ours. For this reason, a comparison can be made in order to determine if they can be used in black skin context. So we calculate them for the same images used to calculate our features values. Like we did for our features, we

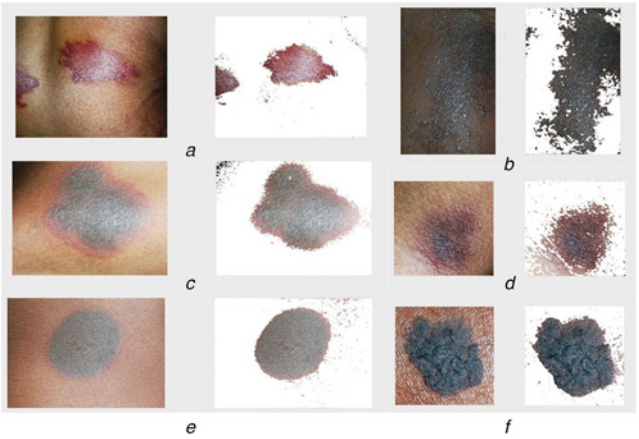

Fig. 3 *Some segmentation results*
a Purpura lesion
b Liquefied eczema
c, d, e Different types erythema
f Seborrheic keratosis

Table 2 Ranges of texture parameters values

Characteristics	Mean	SD	Min	Max
contrast	53.9345	16.223	35.709	61.384
smoothness	0.0479	0.0279	0.0192	0.1526
skewness	−3.9295	5.0623	−4.1789	0.0821
uniformity	0.4698	0.1609	0.2261	0.7360
entropy	2.8415	1.0635	0.8285	4.4567
kurtosis	0.7027	4.4549	0.4138	1.0224

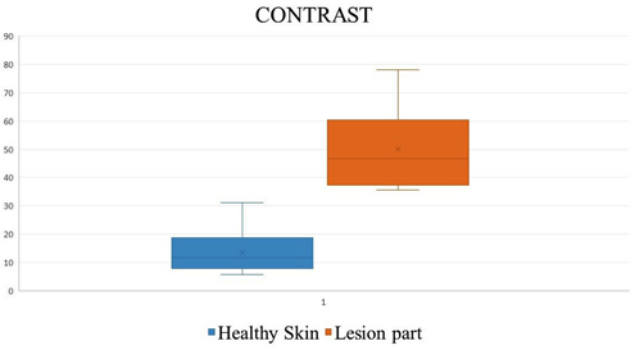

Fig. 4 *Value ranges of contrast respectively for healthy skin and lesion*

doi: 10.1049/htl.2020.0057

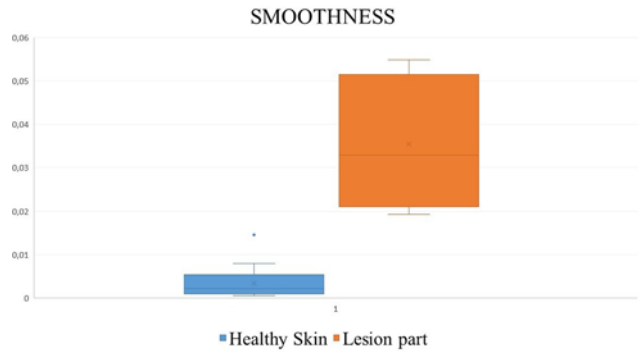

Fig. 5 *Value ranges of smoothness respectively for healthy skin and lesion*

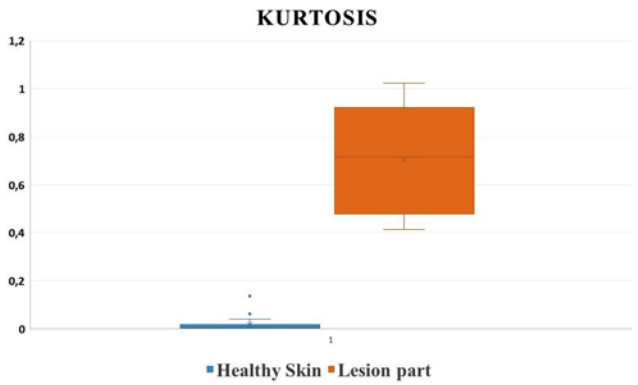

Fig. 6 *Value ranges of kurtosis respectively for healthy skin and lesion*

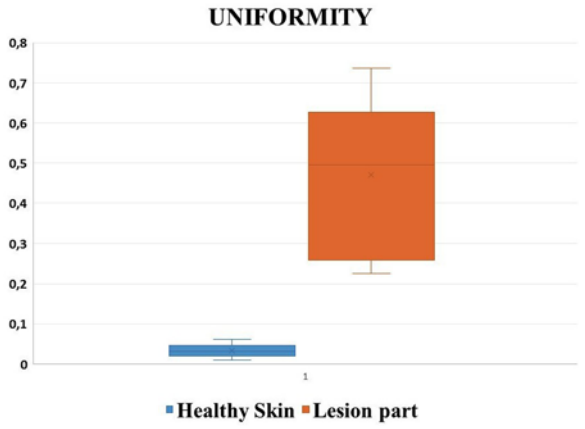

Fig. 7 *Value ranges of uniformity respectively for healthy skin and lesion*

compare values obtained with lesion images to those obtained with healthy skin images. Obtained results are similar for them: Fig. 10 shows results obtained for features F1, F2, F3, F4, F9, F10 and F13 whose formulas and details are explained in [7]. An analysis of boxplots of Fig. 10 can lead to conclude that values calculated for investigated features, for healthy skin images and lesions or pigmented disorders images, respectively, are not in distinct range. This means that these features are not suitable for differentiating healthy skin and pigmented disorders (including lesion) in black skin. These poor results can be explained by the fact that the distinction between limits of the lesion and healthy skin has not been taken into account here when computing these features. However, combined with other features, they could provide a differential diagnostic approach between two types of macular lesions; this may be the subject of future work.

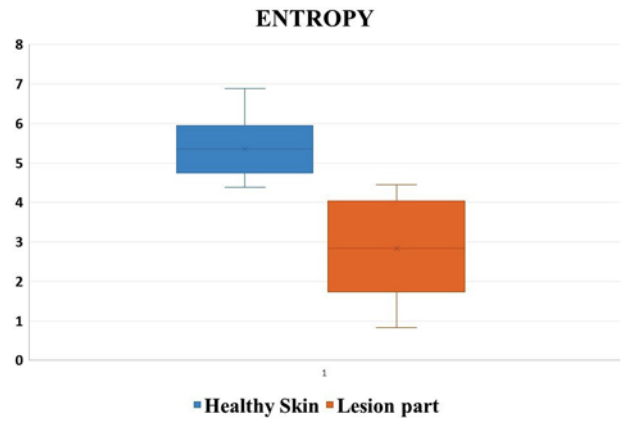

Fig. 8 *Value ranges of entropy respectively for healthy skin and lesion*

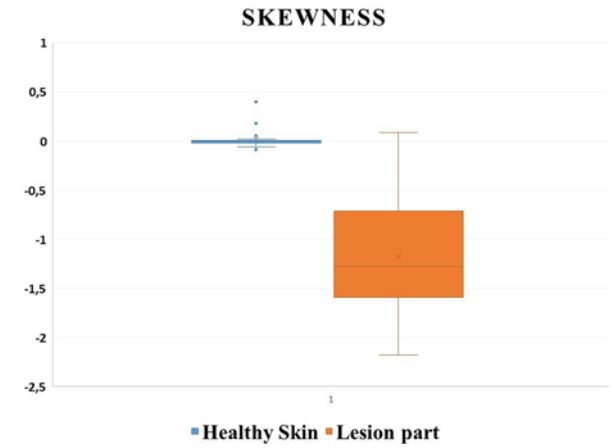

Fig. 9 *Value ranges of skewness respectively for healthy skin and lesion*

Furthermore, for a matter of methods comparison, we implemented our NNFC method on 150 images selected from our database. We also implemented following methods in the same 150 images: adaptive threshold (AT), FBSM, K-means (KM), flux-gradient serpent (GVF), watershed (WTSh) and FCM. The choice of these methods is driven by the fact that they have been identified as being among the most efficient according to comparative studies presented in [17, 19]. Details of these methods can be read in [17–20]. After implementing the methods, we evaluate each of them using following metrics: sensitivity or true positive rate (TPR), specificity (SPC) or true negative rate, false positive rate (FPR), accuracy (Acc), Hausdorff distance (HD) and Hammoude distance (Hm). Their formulas and explanations are detailed in [17]. Metrics values obtained are presented in Table 3 where best performances are in bold font and the worst are in italic font.

From the analysis of Table 3, NNFC is the best of all tested methods since it has the best performance for many metrics. We also noticed that methods are generally less effective on black skin than on white skin. Indeed, when we consider the experimental results obtained for each of them in comparative studies published in [17, 19], we can notice that they are normally more efficient from the point of view of metrics used. For example, in [17], FBSM is the best method followed by the AT method; while according to the results presented in [19], GVF snake method presents the best compromise followed by watershed. From the analysis of Table 3, we can notice that the proposed NNFC method improves the performance of the original FCM method on which it is based.

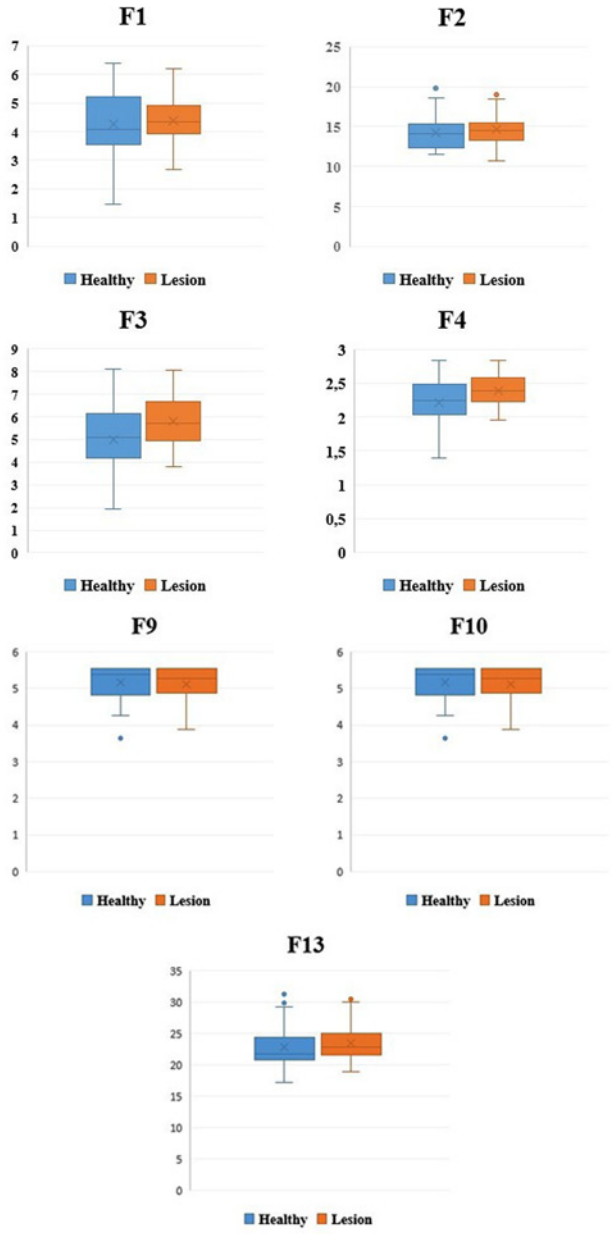

Fig. 10 *Value ranges of features identified in [6, 7]*

Table 3 Comparison of NNFC with other methods

Methods	HD (pixels)	Hm, %	TPR, %	FPR, %	TNR, %	ACC, %
AT	*79.58*	*28.19*	81.16	11.55	*82.71*	80.89
FBSM	76.01	26.32	*77.58*	*22.60*	86.94	*79.49*
KM	57.99	21.21	89.78	7.70	88.71	89.03
GVF	59.04	**13.46**	88.63	8.64	94.25	90.72
FCM	57.54	20.88	91.41	7.42	85.96	90.42
WTSh	66.77	24.58	88.79	8.56	80.19	79.98
NNFC	**54.79**	18.42	**93.81**	**7.34**	**96.53**	**94.67**

6. Conclusion: The purpose of characterisation is to calculate, from images, parameters that can help to identify structures specific to a type of lesion. The characteristics selected in this study are calculated on pixels belonging to the ROI. The experimental results obtained after calculation of the characteristics values in several images show that from one image to another, obtained values are different. We also note that the situation is the same even though it is the same lesion. That said, very close values are noticed for some images. Not having a sufficiently large number of images of each type of lesion, we could not define ranges of values that would allow us to propose an approach of automatic differentiation of lesions between themselves. Other works will focus on this topic.

We also propose in this work a novel approach of black skin lesion images segmentation named NNFC. It consists in firstly

transforming the colour of likely safe skin regions. The selection of these regions is done by an MLP-ANN classifier trained for this purpose and whose learning parameters are mainly texture features. The second step uses the modified FCM clustering method. According to the obtained results, the method is suitable for black skin lesion macroscopic images segmentation. Its relevance has been proved by comparison with other very good existing methods.

This study also revealed significant differences that exist between black skin and white skin and how difficult practising dermatology on black skin is, because of the lack of precise equipment. This state of acts justifies the interest of future research about the development of a computer-assisted diagnostic system dedicated to black skin.

7 References

[1] Azehoun-Pazou G.M., Assogba K.M., Adegbidi H.: 'A novel approach of black skin lesion images segmentation based on MLP neural network'. Proc. IEEE Int. Conf. on Bio-engineering for Smart Technologies (BioSMART), Dubai, UEA, December 2016, pp. 1–4

[2] Carrara M., Bono A., Bartoli C., *ET AL.*: 'Multispectral imaging and artificial neural network: mimicking the management decision of the clinician facing pigmented skin lesions', *Phys. Med. Biol.*, 2007, **52**, (9), p. 2599

[3] Deshabhoina S. V., Umbaugh S. E., Stoecker W. V., *ET AL.*: 'Melanoma and seborrheic keratosis differentiation using texture features', *Skin Res. Technol.*, 2003, **9**, (4), pp. 348–356

[4] Serrano C., Acha B.: 'Pattern analysis of dermoscopic images based on Markov random fields', *Pattern Recognit.*, 2009, **42**, (6), pp. 1052–1057

[5] Tanaka T., Torii S., Kabuta I., *ET AL.*: 'Pattern classification of nevus with texture analysis', *IEEJ Trans. Electr. Electron. Eng.*, 2008, **3**, (1), pp. 143–150

[6] Rundo F., Conoci S., Banna G. L., *ET AL.*: 'Evaluation of Levenberg–Marquardt neural networks and stacked autoencoders clustering for skin lesion analysis, screening and follow-up', *IET Comput. Vis.*, 2018, **12**, (7), pp. 957–962

[7] Conoci S., Rundo F., Petralta S., *ET AL.*: 'Advanced skin lesion discrimination pipeline for early melanoma cancer diagnosis towards PoC devices'. Proc. European Conf. on Circuit Theory and Design (ECCTD), Catania, Italy, 2017, pp. 1–4

[8] Wighton P., Lee T. K., Lui H., *ET AL.*: 'Generalizing common tasks in automated skin lesion diagnosis', *IEEE Trans. Inf. Technol. Biomed.*, 2011, **15**, (4), pp. 622–629

[9] Deng Y., Kenney C., Moore M. S., Manjunath B. S.: 'Peer group filtering and perceptual color image quantization'. In '1999 IEEE International Symposium on Circuits and Systems (ISCAS)' (IEEE, New York, USA, 1999, vol. 4), pp. 21–24

[10] Mahé A.: 'Dermatologie sur peau noire' (Doin, France, 2000, 1st edn.)

[11] Yagou H., Ohtake Y., Belyaev A.: 'Mesh smoothing via mean and median filtering applied to face normals'. In Proc. of IEEE Geometric Modeling and Processing Conf. Theory and Applications, 2002, pp. 124–131

[12] Shin D. H., Park R. H., Yang S., Jung J. H.: 'Block-based noise estimation using adaptive Gaussian filtering', *IEEE Transactions on Consumer Electronics*, 2005, **51**, (1), pp. 218–226

[13] Duda R. O., Hart P. E., Stork D. G.: 'Pattern classification' (John Wiley & Sons, USA, 2012, 2nd edn.)

[14] Moody J., Utans J.: 'Architecture selection strategies for neural networks: application to corporate bond rating prediction', in 'Advances of Neural Information Processing Systems (NIPS)', (MIT Press, USA, 1996)

[15] Bezdek J. C.: 'Models for pattern recognition'. in 'Pattern recognition with fuzzy objective function algorithms' (Springer, USA, 1981), pp. 1–13

[16] Ma L., Staunton R. C.: 'Analysis of the contour structural irregularity of skin lesions using wavelet decomposition', *Pattern Recognit.*, 2013, **46**, (1), pp. 98–106

[17] Silveira M., Nascimento J.C., Marques J.S., *ET AL.*: 'Comparison of segmentation methods for melanoma diagnosis in dermoscopy images', *IEEE J. Sel. Top. Signal Process.*, 2009, **3**, (1), pp. 35–45

[18] Mirkin B.: 'Clustering: a data recovery approach' (CRC Press, USA, 2012, 2nd edn.)

[19] Ferreira P. M., Mendonça T., Rocha P.: 'A wide spread of algorithms for automatic segmentation of dermoscopic images'. Proc. 6th Iberian Conf. on Pattern Recognition and Image Analysis, Funchal, Madeira, Portugal, June 2013, pp. 592–599

[20] Maeda J., Kawano A., Saga S., *ET AL.*: 'Number-driven perceptual segmentation of natural color images for easy decision of optimal result'. Proc IEEE Int. Conf. on Image Processing, San Antonio, Texas, September 2007, vol. 2, pp. I–265